

Trade-offs in Temperature Control of Fast-Ramp RTO and RTA Systems[†]

DICK DE ROOVER, ABBAS EMAMI-NAEINI, JON L. EBERT, AND ROBERT L. KOSUT

SC Solutions Inc.
3211 Scott Boulevard
Santa Clara, CA 95054
USA
roover@scsolutions.com

Abstract

Trade-offs in temperature control of fast-ramp RTP systems from an open-loop-input point of view are investigated, i.e., for a given desired temperature recipe a set of lamp command profiles is determined such that the resulting set of measured temperatures approaches the desired recipe as closely as possible. Exact tracking of fast-ramp recipes with rates such as $250^\circ\text{C}/\text{sec}$ is usually not possible if other performance constraints, such as actuator saturation and/or small temperature overshoot, also have to be met. We investigated these trade-offs for a simulation model of a generic RTP system, both for fast-ramp oxidation (RTO) and fast-ramp spike anneal (RTA) processes.

1 Introduction

Rapid Thermal Processing (RTP) is now becoming part of the mainstream semiconductor manufacturing technology. A typical fabrication process may consist of half a dozen different steps of RTP oxidation (RTO), annealing (RTA), nitridation (RTN) and chemical vapor deposition (RT-CVD). Submicron critical dimensions place stringent demands on thermal processing of wafers. In RTA, both temperature ramp-up and ramp-down rates are important. To minimize diffusion lengths, the amount of time that the wafer is at the processing temperature must be minimized and high temperature ramp rates are desirable. For example, an RTA ramp rate of $400^\circ\text{C}/\text{sec}$ resulted in minimum junction depth [1].

Fast-ramp RTP systems continue to be of interest to the industry for growing thin gate oxides, spike anneals, as well as throughput considerations. From a control point of view, fast ramping is a completely new challenge with problems that have not been encountered before: dynamic behavior—which did not play a role in tracking ramps with low ramp rates—can seriously limit the achievable performance when tracking ramps with high ramp rates. Important issues to deal with are: overshoot, actuator saturation, wafer temperature non-uniformity, and robustness against

high-frequency modeling errors and disturbances.

In a previous paper we considered the limitations of feedback control in tracking fast ramps for a generic RTP system, see [2]. Measurement noise and plant disturbances posed serious limitations on the achievable performance with feedback. Performance improvement was obtained by adding feedforward control and pre-filter to the control scheme. This paper will address the fundamental control limitations of tracking fast ramps for a generic RTP system from an open-loop-input point of view. The thermal dynamics of the system do not allow tracking fast ramps without error if other performance constraints, such as actuator saturation and limited temperature overshoot, have to be met. Typically, trade-offs have to be made between the other requirements and/or constraints.

In a recent paper, we investigated trade-offs in temperature control of fast-ramp RTP systems from an *optimal-control-input* point of view for the generic RTP system, see reference [3]. It was shown that exact tracking of ramps with rates higher than $75^\circ\text{C}/\text{sec}$ violated the actuator limitations. Using the formulation of an optimal trajectory (ramp) redesign problem according to the technique described in [4, 5], it was shown that ramp rates of $150^\circ\text{C}/\text{sec}$ could be tracked that did not violate the actuator constraints and limited overshoot and steady-state tracking error to 1°C . Tracking of ramps with higher ramp rates with less than 1°C overshoot and steady-state tracking error, could only be achieved

[†]Research supported by Defense Advanced Research Projects Agency (DARPA) Applied Computational Mathematics Program under ONR contract N00014-98-C-0201.

if the lamp inputs were redesigned to allow for higher input power.

The results in [3] were generated with a linear model of an RTP system. However, actual RTP systems are highly nonlinear because of the significance of thermal radiation as a mechanism for energy transfer and the large temperature range of operation. In this paper we will investigate the trade-offs for a nonlinear model of a generic RTP system. For this purpose, Iterative Learning Control (ILC) is used to iteratively determine the open-loop lamp power signals that drive the measured RTP outputs along a desired temperature trajectory, see references [12-14]. Using ILC we will determine lamp power inputs both for oxidation (RTO) and annealing (RTA) recipes.

The outline of the paper is as follows. Section 2 describes the RTP plant properties and the derivation of a linear model from a nonlinear model of the generic RTP system. Temperature control performance requirements are described in Section 3. Section 4 briefly summarizes Iterative Learning Control. Section 5 discusses tracking of fast-ramp oxidation processes, while Section 6 investigates fast-ramp spike anneals. Section 7 is conclusions.

2 RTP Plant and Model

The simulation results in this paper are based on a previously derived physical model of the generic RTP system [6-11]. The generic RTP system geometry is shown in Figure 1, which is representative of most modern commercial RTP systems. The system consists of five independently powered lamps near the top wall that form axi-symmetric rings

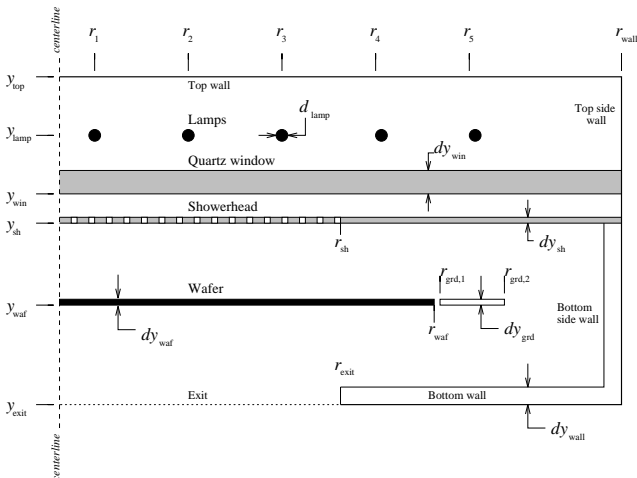


Figure 1: Schematic of the Generic RTP Chamber.

at radii r_1, \dots, r_5 . The walls of the chamber are highly reflective (95%) and water-cooled. A thick quartz window (6.35 mm) and a thinner quartz shower-head (1mm) transmit radiation from the hot lamps at wavelengths shorter than approximately $4\mu\text{m}$, but are opaque to radiation at longer

wavelength. The silicon wafer and guard ring are heated by this short wavelength lamp radiation. A physical model of this nonlinear system was constructed that predicts the dynamic temperature response. Details of this model are described in Ebert et al. [6].

Due to the significance of thermal radiation as a mechanism for transfer of energy in RTP systems and the large temperature range of operation, the system's behavior is highly nonlinear. In addition, these systems are multivariable having multiple temperature sensors (outputs) and multiple lamp groups for actuation (inputs). The generic RTP system has five inputs and five outputs. The individual channels are strongly coupled, i.e., each input has a relatively significant influence on each of the five outputs.

The dynamic range of an RTP system is fairly large due to the large variation in thermal mass and heat transfer of the various components. The lamp filaments are the smallest elements, and hence the fastest. On the other hand, a quartz window has a relatively large thermal mass and is cooled rather poorly, and hence is relatively slow.

For the design of an Iterative Learning Controller later on in this paper a linear model is needed, which will be derived from the simplified nonlinear physical model of the generic RTP chamber [6]. Let the simplified nonlinear model be given by:

$$\begin{aligned} \dot{x} &= f(x) + B_1 u \\ y &= h(x). \end{aligned}$$

Here $f(x)$ and $h(x)$ are nonlinear functions of the state x , and y are the sensor outputs. By selecting a suitable linearization (operating) point (x_o, u_o) a linear model can be derived by computing:

$$\begin{aligned} A &= \left. \frac{\partial f}{\partial x} \right|_{x_o} \\ B &= B_1 \\ C &= \left. \frac{\partial h}{\partial x} \right|_{x_o} \end{aligned}$$

resulting in the linear model:

$$\begin{cases} \dot{\tilde{x}} &= A\tilde{x} + B\tilde{u} \\ \tilde{y} &= C\tilde{x} \end{cases} \quad (1)$$

An important issue in the linearization is the selection of the linearization point (temperature).

3 Performance Requirements

Wafer quality is explicitly determined by the temperature control performance of the RTP chamber. In this paper we impose the following requirements on the RTP temperature control in order to ensure good wafer quality:

- Steady-state tracking error should be less than 1°C .
- Overshoot should be less than 1°C for temperature changes up to 600°C , ramp-rates up to 250°C , and setpoints up to 1100°C .

Furthermore, we deal with the following actuator constraints:

- Normalized power is limited to 1 (lamps full on).
- Normalized power cannot be negative (lamps off).

In this paper we will investigate tracking of ramps with rates 50° , 150° and 250°C/sec , respectively, for a temperature setpoint change from 600°C to 1100°C .

4 Iterative Learning Control

Consider the configuration depicted in Figure 2. The main

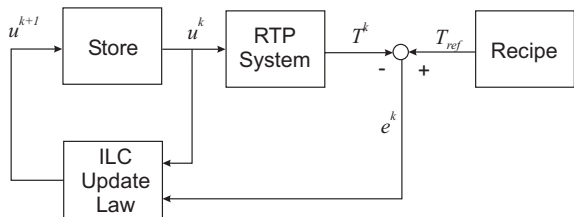


Figure 2: Blockscheme of Iterative Learning Control for RTP.

idea of iterative learning control is to iteratively *update* the signal u , so as to *decrease* the magnitude of the temperature tracking error e^k , after each cycle of the reference signal T_{ref} , see e.g. [12-14]. More formally, let k denote the number of iterations, then ILC deals with finding an update U of the signal u at the k th iteration, based on the temperature tracking error at the k th iteration, i.e.,

$$u^{k+1}(t_j) = U(u^k(t_j), e^k(t_j)), \quad t_j \in [0, T_N], \quad k \in N, \quad (2)$$

such that

$$\lim_{k \rightarrow \infty} u^k(t_j) = u^*(t_j) \quad \text{and} \quad \lim_{k \rightarrow \infty} \|e^k(t_j)\| = e^*,$$

with $u^*(t_j)$ and e^* being fixed points, and e^* is minimal over the interval $[0, T_N]$, which is defined as: $[0, T_N] \doteq [t_0, t_{\Delta T}, \dots, t_{N\Delta T}]$, and e^* is measured in some signal norm $\|\cdot\|$. Obviously, convergence of an ILC scheme to fixed points u^* and e^* , depends on the choice of the update law (2); the great body of literature on ILC mainly concerns ‘newly’ proposed update laws. Roughly speaking, for linear systems two different types of update laws can be distinguished: a *Proportional Integral Derivative* (PID)-type of

update law and a *model-based* update law. The most general PID-type of update law can be found in [12], which updates the input according to:

$$u^{k+1}(t) = u^k(t) + \alpha e^k(t) + \beta \dot{e}^k(t) + \gamma \int e^k(t) dt. \quad (3)$$

For this type of ‘learning’ rule, convergence conditions are derived, so as to obtain the gains $\{\alpha, \beta, \gamma\}$.

The most general model based update law is proposed in [13], and reads as follows:

$$u^{k+1}(t_j) = Q(q)u^k(t_j) + L(q)e^k(t_j). \quad (4)$$

Here q is the forward shift operator defined as: $qt_j = t_{j+1} = t_j + \Delta T$, with ΔT being the sampling interval. General convergence conditions on the filters Q and L are derived, based on knowledge (i.e., a model) of the system. In fact, update law (4) can be seen as a generalization of update law (3), by making specific choices of the filters Q and L . Hence, we will only consider learning rule (4).

A general design method for the filters Q and L can be found in [14]. Here we choose the L filter equal to the dynamic inverse of the linear plant model that was derived in Section 2, and the Q filter as a low-pass filter; the cut-off frequency of the low-pass filter can be used as a design parameter to trade-off exact tracking vs temperature uniformity, as will be shown later in this paper.

Henceforth, all simulated lamp power inputs will be determined by applying a learning iteration such that the difference between two successive iterations is within a sufficiently small tolerance. A typical learning iteration converges within 10 iterations.

Figure 4 shows such a typical iteration for an oxidation recipe with ramp-up rate of 250°C/sec . Using an optimization procedure, we computed the steady-state lamp commands that hold the system temperatures at 600°C such that the simulated measured temperatures start with zero error. Since the L filter is equal to the dynamic inverse of a *linear* plant model—which is acquired at only *one* temperature operating point—the (steady-state) error at iteration 0 is more than 150°C , see first row in Figure 4. However, in the 1st iteration the error has been reduced to less than 40°C (2nd row in Figure 4) and in the 2nd iteration the error at steady-state is almost zero (3rd row, 2nd column). At iteration 5 the error has converged almost to its final value, which can be seen from the small difference between iteration 5 and 10 (4th and 5th row in Figure 4, respectively). Note the difference in steady-state lamp commands between iteration 0 and iteration 10 (column3, rows 1 and 5, respectively): the steady-state lamp commands after convergence (iteration 10) are the values that are needed to hold the measured temperature at 1100°C . The slow drift in the lamp commands is due to the slow heating of the quartz window.

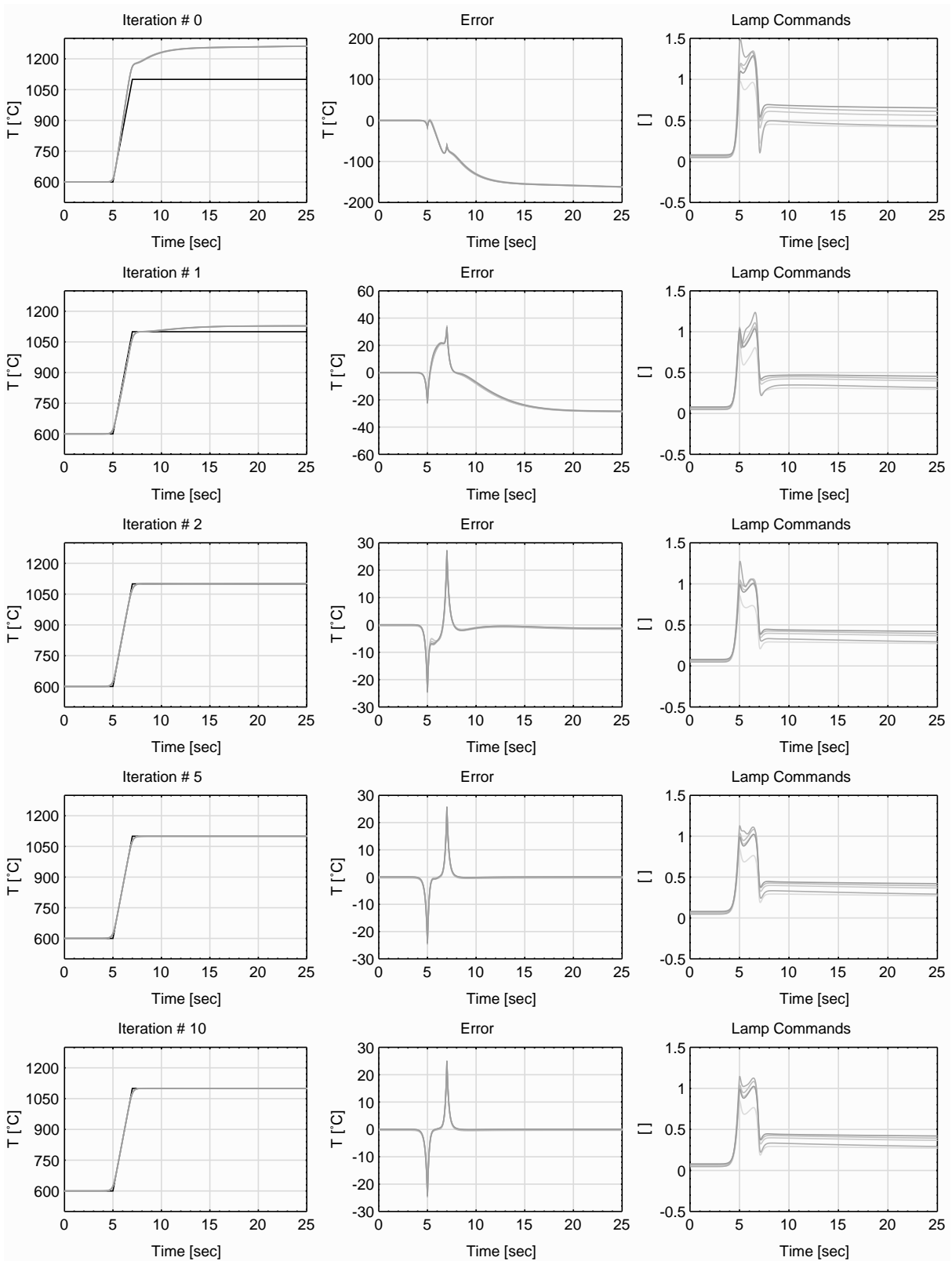


Figure 3: Typical sequence of ILC iterations. This iteration was performed for an oxidation recipe with ramp-up rate of 250° C/sec. Each row in the left column shows the recipe and the simulated temperature measurements for one iteration; the middle column shows the difference between the recipe and the measured temperatures, and the right column shows the corresponding lamp commands.

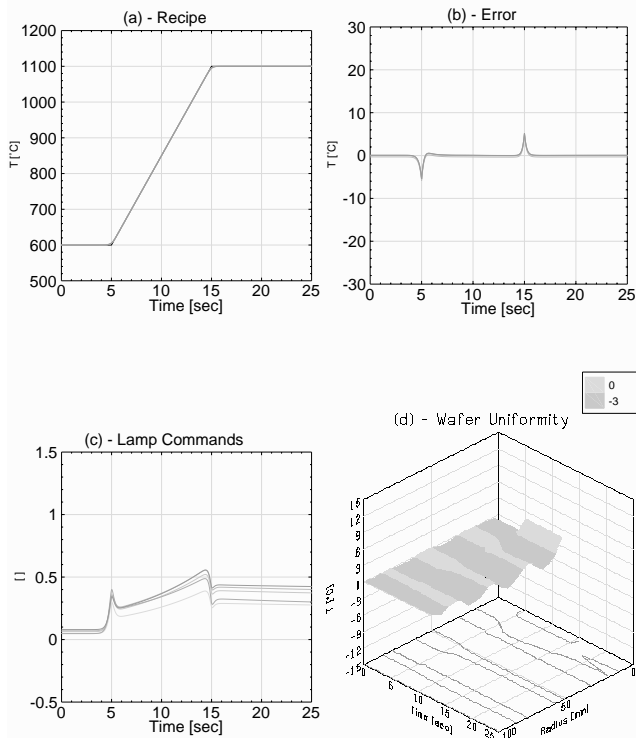


Figure 4: Simulation results for exact tracking of an oxidation recipe with ramp-up rate of 50° C/sec . (a) Desired recipe T_{ref} and simulated measured temperatures $T_i, i = 1 \dots 5$; (b) Difference between T_{ref} and $T_i, i = 1 \dots 5$; (c) Corresponding normalized lamp power inputs; (d) Wafer temperature non-uniformity with respect to the wafer center temperature; center = 100 mm.

5 Tracking of Fast-Ramp Oxidation Processes

It is important to investigate what lamp power inputs are needed to exactly track fast-ramp oxidation recipes for the generic RTP system. We will investigate exact tracking for recipes with ramp-up rates of 50° , 150° and 250° C/sec , respectively. Figure 4 shows exact tracking of a recipe with ramp-up rate of 50° C/sec .

Figure 4(a) shows the recipe together with the simulated measured temperatures (5 signals) after convergence of the ILC iteration. Figure 4(b) shows the difference between the recipe and each of the 5 measured temperatures. Figure 4(c) shows the corresponding lamp commands, and Figure 4(d) shows the wafer temperature non-uniformity. The surface represents the temperature non-uniformity with respect to the wafer center temperature as a function of time and wafer radius; the left horizontal scale is time in seconds, the right horizontal scale is wafer radius in millimeter (100 mm is wafer center, and 0 mm is wafer edge), and the vertical scale is temperature in $^\circ \text{ C}$.

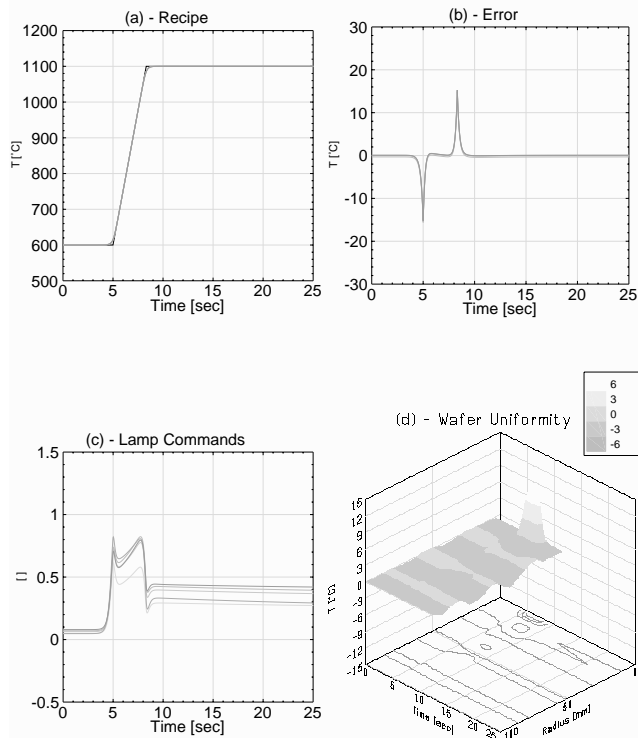


Figure 5: Simulation results for exact tracking of an oxidation recipe with ramp-up rate of 150° C/sec . (a) Desired recipe T_{ref} and simulated measured temperatures $T_i, i = 1 \dots 5$; (b) Difference between T_{ref} and $T_i, i = 1 \dots 5$; (c) Corresponding normalized lamp power inputs; (d) Wafer temperature non-uniformity with respect to the wafer center temperature; center = 100 mm.

An immediate problem in *exact tracking* of ramp profiles shows up in Figure 4(b) where sharp pulses occur in the tracking error $T_{ref} - T_i, i = 1 \dots 5$. Each channel of the RTP model consists of a series/parallel connection of three first order systems. Hence, the inverse plant differentiates the input once, twice or three times, depending on the frequency range. This means that exact tracking of T_{ref} can be obtained only if T_{ref} is one, two or three times differentiable, and depends solely on the frequency spectrum of T_{ref} and the corresponding frequency response of the plant. The recipe T_{ref} can only be differentiated twice, resulting in a pulse input. However, a pulse input is not desirable because it saturates the lamps and might even damage them.

To prevent pulse inputs, we filtered the recipe with a second-order low-pass filter with relative damping equal to 1 and natural frequency at approximately 1.5 Hz. This rounds-off the sharp corners of the ramps, as can be inferred from the simulated outputs in 4(a). Also, the cut-off frequency of the Q filter, which filters the lamp power inputs, was chosen equal to this frequency. The corresponding lamp power inputs that provides exact tracking of this pre-filtered ramp are shown in Figure 4(c). As expected, there are no sharp pulses in the input signals. Instead, a pulse-like tracking error remains in Figure 4(b).

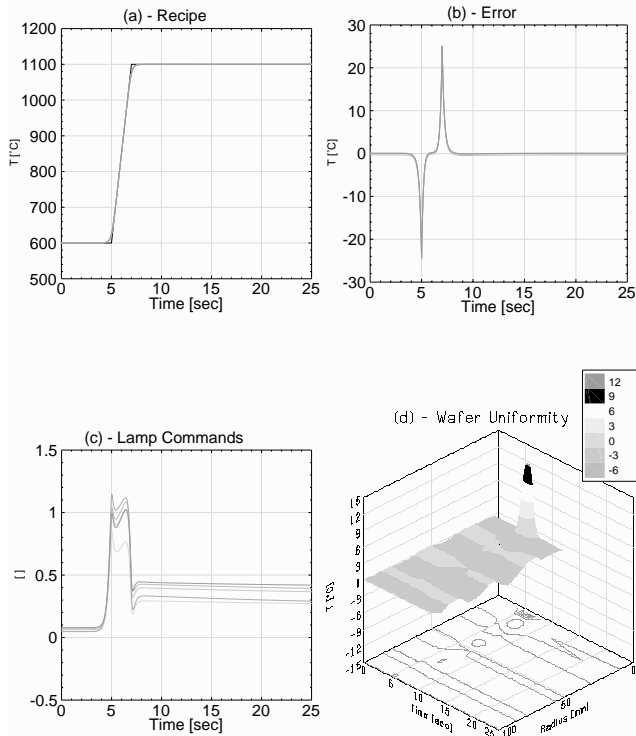


Figure 6: Simulation results for exact tracking of an oxidation recipe with ramp-up rate of $250^{\circ}\text{C}/\text{sec}$. (a) Desired recipe T_{ref} and simulated measured temperatures $T_i, i = 1 \dots 5$; (b) Difference between T_{ref} and $T_i, i = 1 \dots 5$; (c) Corresponding normalized lamp power inputs; (d) Wafer temperature non-uniformity with respect to the wafer center temperature; center = 100 mm.

Figures 5 and 6 show the simulated tracking results for ramps with rates 150° and $250^{\circ}\text{C}/\text{sec}$, respectively. Note again that we pre-filtered the ramps with the 2nd order low-pass filter in order to create a 3 times differentiable reference.

It can be seen from these figures that exact tracking of a ramp with rate $250^{\circ}\text{C}/\text{sec}$, requires lamp command inputs that exceed the actuator limit of 1. Gradually increasing the ramp rate from $150^{\circ}\text{C}/\text{sec}$ shows that the actuator saturation limit is reached for a rate of approximately $210^{\circ}\text{C}/\text{sec}$. This clearly indicates that exact tracking of fast ramps with rates higher than $210^{\circ}\text{C}/\text{sec}$ is not possible unless a trade-off is made in the tracking requirement.

Comparison of Figures 4(d) to 6(d) shows increased wafer temperature non-uniformity at the edge of the wafer with increased ramp-rate. This is due to the fact that the guarding is slowing down the heating of the edge of the wafer. This effect becomes more prominent as speed of heating (i.e., ramp-rate) increases.

Figure 7 shows the simulation results for tracking of an oxidation recipe with ramp-up rate of $250^{\circ}\text{C}/\text{sec}$ with normalized lamp power commands limited between 0 and 1.

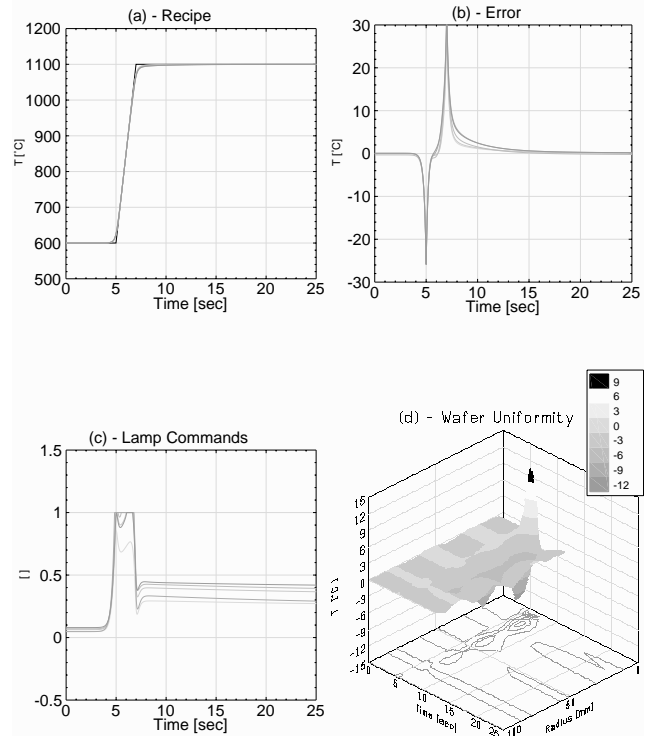


Figure 7: Simulation results for tracking of an oxidation recipe with ramp-up rate of $250^{\circ}\text{C}/\text{sec}$ and lamp power saturation. (a) Desired recipe T_{ref} and simulated measured temperatures $T_i, i = 1 \dots 5$; (b) Difference between T_{ref} and $T_i, i = 1 \dots 5$; (c) Corresponding normalized lamp power inputs; (d) Wafer temperature non-uniformity with respect to the wafer center temperature; center = 100 mm.

Although tracking is achieved during ramp-up, the sharp corner cannot be negotiated quickly enough and consequently the system's response has undershoot. Moreover, the measured temperature uniformity is degraded, see Figure 7(b), and makes wafer temperature uniformity even worse, see Figure 7(d).

One way to improve the wafer uniformity is to prevent the lamp power commands from saturating. This can be accomplished by lowering the cut-off frequency of the ILC Q -filter and, correspondingly, the cut-off frequency of the recipe smoothing filter. Figure 8 shows the results for a cut-off frequency of 0.5 Hz; the cut-off was chosen at 0.5 Hz because at that frequency the lamp commands had a maximum value right at the saturation limit, see Figure 8(c). Figures 8(a) and (b) show that tracking (large temperature tracking error) has been traded-off versus improved uniformity (measured temperatures close together). Figure 8(d) shows the improved wafer temperature uniformity. Basically, the temperature uniformity of the unconstrained-lamp-command simulation has been recovered, compare Figure 8(d) with Figure 6(d).

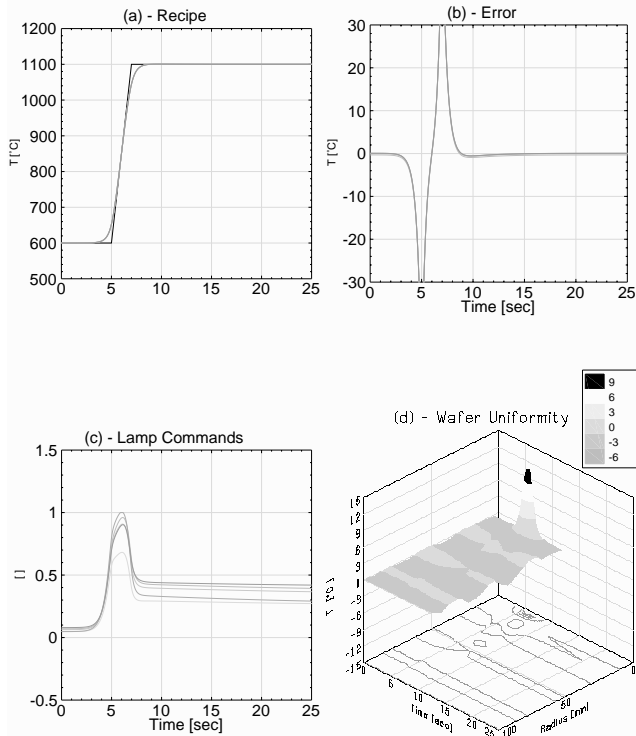


Figure 8: Simulation results for tracking of an oxidation recipe with ramp-up rate of $250^{\circ}\text{C}/\text{sec}$ with lamp power saturation and smooth cut-off. (a) Desired recipe T_{ref} and simulated measured temperatures $T_i, i = 1 \dots 5$; (b) Difference between T_{ref} and $T_i, i = 1 \dots 5$; (c) Corresponding normalized lamp power inputs; (d) Wafer temperature non-uniformity with respect to the wafer center temperature; center = 100 mm.

6 Tracking of Fast-Ramp Spike Anneal Processes

In spike anneal processes both temperature ramp-up and ramp-down rates are important, as the amount of time that the wafer is at processing temperature must be minimized so as to minimize the diffusion lengths. Therefore, both ramp-up and ramp-down rate have to be as high as possible.

Figure 9 shows tracking without trade-offs of a fast-ramp spike anneal recipe with ramp-up rate of $250^{\circ}\text{C}/\text{sec}$ and ramp-down rate of $50^{\circ}\text{C}/\text{sec}$. The ramp-down rate of $50^{\circ}\text{C}/\text{sec}$ is a trade-off between temperature uniformity and actuator saturation: as can be seen from Figure 9(c), the lamps start saturating low at time $t \approx 13$ sec. As soon as the lamps saturate, temperature uniformity is lost, see Figures 9(b) and (d). For ramp-down rates higher than $50^{\circ}\text{C}/\text{sec}$, temperature uniformity is lost earlier, i.e., at a temperature closer to the process temperature of 1100°C ; this is undesirable.

The duration of the recipe at process temperature of 1100°C is chosen as 1 second. This is the minimum time that is needed for the temperatures to hit the process temperature and to ramp down immediately; for smaller soak times,

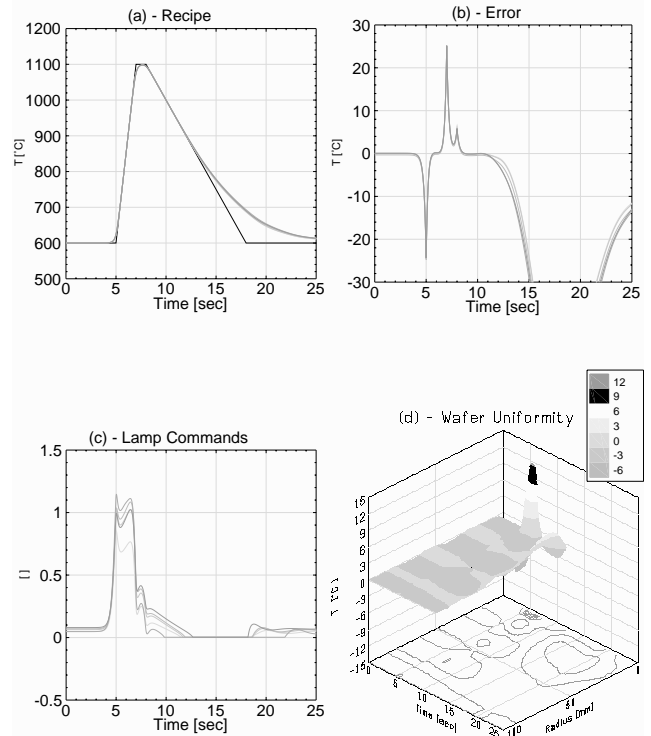


Figure 9: Simulation results for exact tracking of a spike anneal recipe with ramp-up rate of $250^{\circ}\text{C}/\text{sec}$ and ramp-down rate of $50^{\circ}\text{C}/\text{sec}$. (a) Desired recipe T_{ref} and simulated measured temperatures $T_i, i = 1 \dots 5$; (b) Difference between T_{ref} and $T_i, i = 1 \dots 5$; (c) Corresponding normalized lamp power inputs; (d) Wafer temperature non-uniformity with respect to the wafer center temperature; center = 100 mm.

the simulated measured temperatures do not reach the process temperature of 1100°C anymore, but rather approach a lower value.

Again, the normalized lamp commands exceed the limit of 1 for a ramp-up rate of $250^{\circ}\text{C}/\text{sec}$, which is not surprising as the first part of the anneal recipe (up to time $t = 8$ sec.) is exactly equal to the oxidation recipe shown in Figure 6. Figure 10 shows the simulated tracking response of this anneal recipe when lamp commands are limited between 0 and 1. The clipping of the lamp commands have again a significantly negative effect on the wafer temperature uniformity, see Figures 10(b) and (d). Also, the tracking property is lost as the measured temperatures do not reach the process temperature of 1100°C anymore, see Figures 10(a) and (b). This could be solved by increasing the duration of the recipe at process temperature, e.g. from 1 to 1.2 sec (not shown in Figure).

To solve the temperature non-uniformity problem, we again decreased the cut-off frequency of the learning Q filter to 0.5 Hz, and, correspondingly, the cut-off of the recipe-filtering filter. The simulation results are shown in Figure 11. Similar to the oxidation recipe, the temperature uniformity has improved at the cost of a large tracking error. However, for

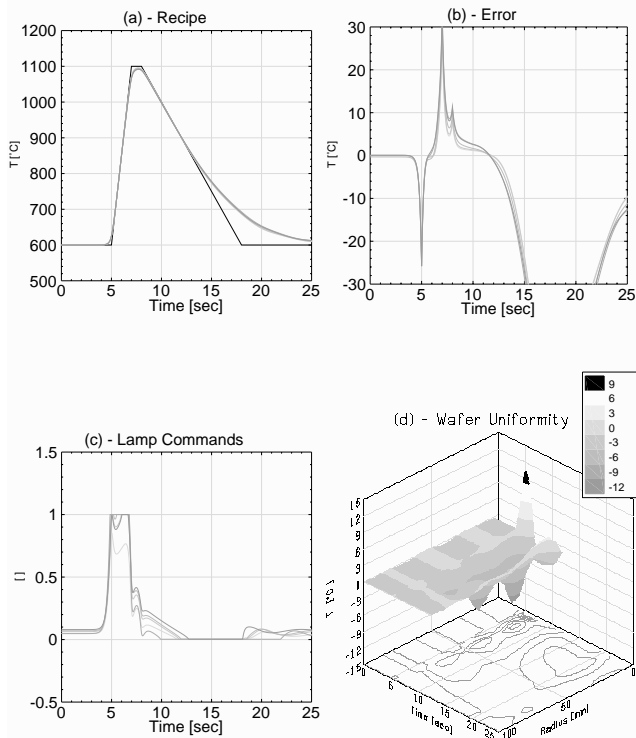


Figure 10: Simulation results for exact tracking of a spike anneal recipe with ramp-up rate of 250° C/sec, ramp-down rate of 50° C/sec, and with lamp power saturation. (a) Desired recipe T_{ref} and simulated measured temperatures $T_i, i = 1 \dots 5$; (b) Difference between T_{ref} and $T_i, i = 1 \dots 5$; (c) Corresponding normalized lamp power inputs; (d) Wafer temperature non-uniformity with respect to the wafer center temperature; center = 100 mm.

this anneal recipe, the large tracking error has the consequence of not reaching the process temperature at all, but a temperature some 25° C lower. To solve this problem, the duration of the soak period at process temperature has to be increased by almost 1 second, which means almost a doubling of the process time. An alternative would be to lower the ramp-up rate to approximately 210° C/sec to prevent lamp saturation.

This clearly shows the trade-offs that have to be made:

- high ramp-up rate vs lamp saturation;
- high ramp-up and ramp-down rate vs temperature uniformity;
- temperature uniformity vs soak time at process temperature;
- lamp saturation vs temperature uniformity;
- lamp saturation vs tracking (smoothness of lamp commands).

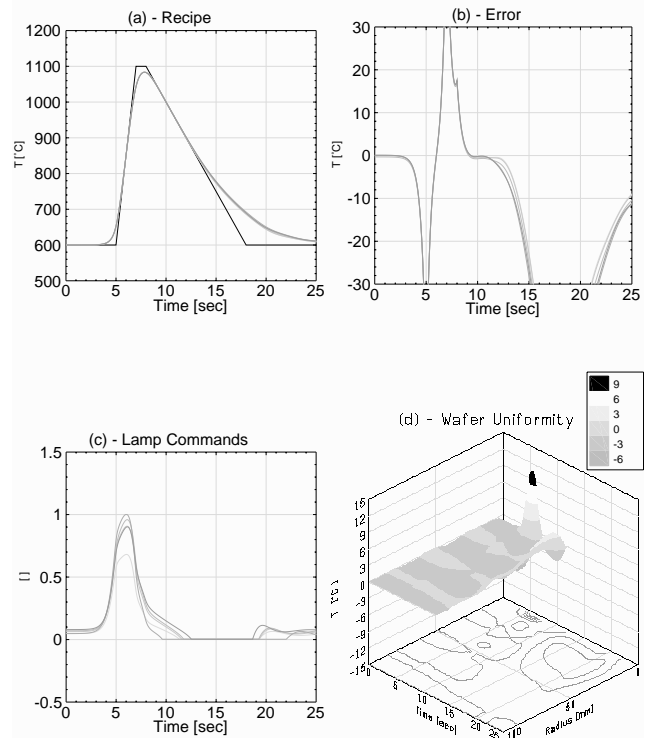


Figure 11: Simulation results for exact tracking of a spike anneal recipe with ramp-up rate of 250° C/sec, ramp-down rate of 50° C/sec, lamp power saturation and smooth cut-off. (a) Desired recipe T_{ref} and simulated measured temperatures $T_i, i = 1 \dots 5$; (b) Difference between T_{ref} and $T_i, i = 1 \dots 5$; (c) Corresponding normalized lamp power inputs; (d) Wafer temperature non-uniformity with respect to the wafer center temperature; center = 100 mm.

All these trade-offs are correlated with each other, which means that the process engineer has the availability of several different “knobs” to reach his goal. The knobs that we used here are:

- ramp-up and ramp-down rates;
- duration of process soak time;
- cut-off frequency of ILC Q -filter and recipe filter.

Other knobs that might be available are:

- choice of different lamps to change maximum lamp power;
- choice of recipes with more than one ramp-up and ramp-down rate, i.e. change of ramp rate during ramp-up and/or ramp-down;
- choice of different process temperatures.

7 Conclusions

In this paper we investigated trade-offs in open-loop temperature control of fast-ramp RTP systems for a simulation model of a generic RTP system. We investigated trade-offs both for fast-ramp oxidation (RTO) and fast-ramp spike anneal (RTA) processes. The simulation results showed that lamp saturation severely affects wafer temperature uniformity, which is unacceptable in many cases. To improve wafer temperature uniformity, perfect tracking can be sacrificed by frequency-band limiting (filtering) both the recipe and the lamp commands. An alternative trade-off would be to lower the maximum ramp rates, or, in case of spike anneals, to increase the process soak time. Spike anneals are more affected by lamp saturation than oxidation processes, since saturation increases either the amount of time that the wafer is at the processing temperature or destroys the wafer temperature uniformity.

One way to implement the results shown in this paper, is for each recipe to store the corresponding lamp commands in feedforward look-up tables, and read-out these tables during operation of the real RTP system. Two additional steps are required when pursuing this method. Firstly and most importantly, a good model of the RTP is needed. Secondly, since even the best model is an approximation of the real system, a feedback controller has to be used in conjunction with the feedforward look-up table, see reference [2] on how to implement feedforward in conjunction with feedback.

References

- [1] S. Shishiguchi, A. Mineji, T. Hayashi, and S. Saito, "Boron Implanted Shallow Junction Formation by High-Temperature /Short-Time/High-Ramping-Rate (400°C/sec) RTA," *Symposium on VLSI Technology Digest of Technical Papers*, pp. 89-90, 1997.
- [2] Roover, D. de, A. Emami-Naeini, J.L. Ebert, S. Ghosal, G.W. van der Linden, "Model-Based Control of Fast-Ramp RTP Systems," *6th International Rapid Thermal Processing Conference*, Kyoto, Japan, 1998.
- [3] Roover, D. de and S. Devasia, "Trade-offs in Temperature Control of Fast-Ramp RTP Systems," in *Proc. 1999 American Control Conf.*, San Diego CA, pp.76-80, 1999.
- [4] Devasia, S. "Optimal Output Trajectory Redesign for Invertible Systems", *J. Guidance, Contr. and Dyn.*, vol.19(5), pp. 1189-1191, 1996.
- [5] Dewey, J.S., K. Leang and S. Devasia "Experimental and Theoretical Results in Output-Trajectory Redesign for Flexible Structures", *ASME J. Dyn. Systems, Meas. and Contr.*, vol.120(4), pp. 456-461, 1998.
- [6] J.L. Ebert, A. Emami-Naeini, R.L. Kosut, "Thermal Modeling of Rapid Thermal Processing Systems," *3rd International Rapid Thermal Processing Conference*, R.B. Fair, B. Lojek (eds), pp. 343-355, Amsterdam, The Netherlands, 1995.
- [7] J.L. Ebert, A. Emami-Naeini, R.L. Kosut, "Thermal Modeling and Control of Rapid Thermal Processing Systems," in *34th IEEE Conf. Decision and Control*, December 1995.
- [8] M. Refai, J.L. Ebert, A. Emami-Naeini, and R.L. Kosut, "RTP Robust Control Design, Part I: Sensitivity Analysis," *4th International Rapid Thermal Processing Conference*, Boise, Idaho, September 1996.
- [9] G.W. van der Linden, J.L. Ebert, A. Emami-Naeini, and R.L. Kosut, "RTP Robust Control Design : Part II Controller Synthesis," *4th International Rapid Thermal Processing Conference*, Boise, Idaho, September 1996.
- [10] H. Aling, R.L. Kosut, A. Emami-Naeini, J.L. Ebert, "Nonlinear Model Reduction with Application to Rapid Thermal Processing," in *Proc. 35th IEEE Conf. Decision and Control*, pp. 4305-4310, Kobe, Japan, December 1996.
- [11] H. Aling, S. Banerjee, A.K. Bangia, V. Cole, J.L. Ebert, A. Emami-Naeini, K.F. Jensen, I.G. Kevrekidis, S. Shvartsman, "Nonlinear Model Reduction for Simulation and Control of Rapid Thermal Processing Systems", in *Proc. American Control Conference*, pp. 2233-2238, June 1997.
- [12] Arimoto, S., "Mathematical Theory of Learning with Applications to Robot Control", in *Proc. 4th. Yale Workshop on Applications of Adaptive Systems*, New Haven, CT, pp.379-388, 1985.
- [13] Moore, K.L., M. Dahleh and S.P. Bhattacharyya, "Iterative Learning Control: A Survey and new Results", *J. Robotic Systems*, vol.9(5), pp.563-594, 1992.
- [14] Roover, D. de, *Motion Control of a Wafer Stage – A Design Approach for Speeding Up IC Production*, PhD Thesis, Mech. Eng. Systems and Control Group, Delft Univ. of Technology, The Netherlands, ISBN 90-407-1562-9/CIP, 1997.